01 Sep 1969

The Structure of a Turbulent Water Jet

Philip J. Morris

THE STRUCTURE OF A TURBULENT WATER JET

Philip J. Morris
The Institute of Sound and Vibration
University of Southampton, England

ABSTRACT

Experimental studies are made to determine the structure of a turbulent water jet.

The paper is divided into two parts. The first gives practical information about the techniques and instrumentation developed to make measurements with hot-wire anemometers in water. A short theoretical discussion is given on the dynamic response of heated fibre in liquids. The second part reports on the results obtained in a one-inch water jet at Reynolds numbers between 12,000 and 20,000. Mean axial velocity measurements are made in the initial five diameters of the jet and the results are used to predict the nature of the vortex shed at the jet lip. Spectrum measurements are made in the same position using an analogue to digital converter and computer to process the data.

The measurements are discussed in relation to the structure of the jet and the formation of vortices at the jet lip.

INTRODUCTION

The disturbances in a jet flow can be of two kinds. Firstly potential disturbances such as pressure fluctuations, density variations, or the irrotational motion of the fluid. Secondly, rotational disturbances connected with fluid shear. Little is known of the interaction between potential and rotational fields and the effect of their coupling. Measurements made with hot-wire anemometers contain both potential and rotational components and the two are indistinguishable without the use of complicated sampling techniques. The report sets out to investigate the result of reducing the order of magnitude of the compressibility effects in the potential disturbances.

A study of the flow properties of a water jet has been made using a hot-wire anemometer specially modified for work in water. The water jet had the advantage of producing a high Reynold's number flow with a very small Mach number. This meant that the compressibility effects, compared with those in an air jet at an equivalent Reynolds number, were almost negligible. In the experiments described the Mach number of the jet exit velocity was varied between 3×10^{-4} and 6×10^{-4} whilst the Reynolds number varied from 13,000 to 20,000. For an equivalent Mach and Reynolds number in air the jet exit diameter would have to be in excess of two meters.

Experiments at the Institute of Sound and Vibration Research have been under way for some time to collect data on a wide range of shear flows. Studies have been made of air-jets to determine both velocity and pressure fluctuations and the related correlations, spectra and probability distributions.[1,2,3] The data obtained from these experiments have been used to provide the comparison with the water-jet results. The velocity and spectrum measurements made in the water jet are used to suggest a structure for the turbulent water jet. The formation of vortex rings in the water jet is discussed in relation to the magnitude of compressible effects.

The instrumentation and techniques required to make measurements with hot-wires and hot-films in water are of fundamental interest to workers engaged in research in liquid flows. Civil engineering problems such as silting in channels, oceanographic research, and other engineering applications have proved it necessary to provide a better understanding of the properties of these instruments when they are being used in water.

For this reason this report is divided into two parts. The first deals with the techniques required to overcome problems connected with electrolysis, dirty liquids and ambient temperature changes when using hot-wires in water. A short theoretical analysis of the dynamic response of hot-films in water, which is known not to be constant, is also included in this part. The second part of the report gives the experimental results obtained by applying these techniques to measurements in a turbulent water jet.

HOT-WIRE ANEMOMETERS IN WATER

The possibility of adapting the hot-wire anemometer for use in liquids has always been an attractive one because of the ease of interpretation of results compared with those of the hot-film and because of the cheapness of producing hot-wire probes compared with hot-film probes. The use of the hot-wire in water was first reported by Gandaghran[4] in 1931. The practical problems involved were discussed by Worster[5] in 1948. It should be remembered the dimensions involved and the voltages used at this time were considerably larger than those used today. The formation of bubbles on the wire occurred when the wire was both insulated and uninsulated usggesting that both electrolysis and water boiling were present. The bubbles were used by Jones[6] in 1959 to clean the wire. An extensive investigation of the use of the hot-wire anemometer in water has been made by Delleur et al.[7] in 1966.

The main difficulties involved in this technique are the drift in calibrations caused by deposits on the wire, the formation of bubbles on the wire by electrolysis and boiling and the problems produced by changes in the liquid temperature. The electrolysis problem can be solved by using very pure, de-ionised water. The presence of small fibres and lint in the water can also be a problem as they can easily catch around the wire causing damage. If it is impossible to work in a dust-free atmosphere, which would precent deposition of particles into the water, then, by using a relatively thick wire, 9 microns diameter say, the particles can be removed by tapping the probe support or by cleaning the wire with a camel-hair brush. If the wire is kept at too high a temperature then bubbles can be produced by boiling. Wire temperature was kept only 20°C above ambient in these experiments so boiling effects were eliminated. Because of this low wire to ambient temperature ratio, variations in the fluid temperature can cause larger changes in the anemometer output than do velocity variations. A number of systems have been developed by the author[8] to compensate for changes in ambient temperature with a frequency of up to one cycle per second. The compensation systems developed include an open-loop system

using a directly-heated thermistor as a temperature sensor and a closed-loop system using a cold-run wire as the sensor. Using these techniques a steady calibration of the wire was obtained.

The wire calibration curve, figure 1, follows approximately a one-sixth power law. This agrees with the theoretical prediction by the author.[9]

FREQUENCY RESPONSE OF HEATED FILMS

The steady-state calibration of hot-film probes cannot be used to determine the dynamic sensitivity when working in air. This has been shown by Bankoff and Rosler.[10] In his work on the theoretical frequency response of thin film thermometers, Fabula,[11] considered the heated film to be at the stagnation point of the probe. The stagnation flow method is used below to obtain the frequency response of hot-film gauges.

The theoretical model is set up as in figure 2 with the fluid approaching the film in the negative y-direction. It is assumed that the film is kept at a steady mean temperature with a harmonic fluctuating heating superimposed. The equations of motion for the two regions may be written as:

In the fluid $$\frac{\partial T}{\partial t} + (\bar{q}\cdot\nabla)T = D_f \nabla^2 T$$

In the substrate $$\frac{\partial T}{\partial t} = D_s \nabla^2 T$$

where D_f and D_s are the thermal diffusivities in the fluid and substrate, respectively.

If we write $$T = \underline{\underline{\theta}} + \theta e^{i\omega t}$$

The boundary conditions are;

$$y = 0 \qquad \underline{\underline{\theta}} = T_o$$

and $$\theta = T_1$$

With the assumption of an infinite substrate, as considered by Fabula, the fluctuating heat transfer to the substrate, q_{1G} is given by,

$$q_{1G} = -T_1 k_s (1+i)(2\omega/D_s)^{\frac{1}{2}}$$

where k_s and k_f are the thermal conductivities in the substrate and fluid, respectively.

Considering two dimensional flow approaching the wall we have, from Curle,[12] that the velocity distribution is given by

$$u = \beta_1 \frac{x}{c} f'(\eta), \qquad v = -\left(\frac{\nu\beta_1}{c}\right)^{\frac{1}{2}} f(\eta)$$

where the external velocity may be written as $u_1 = \beta_1 x/c$ and $\eta = \left(\frac{\beta_1}{\nu c}\right)^{\frac{1}{2}} y$.

The steady heat transfer from a heated wall in stagnation flow is given by Curle as

$$q_o = k_f T_o \left(\frac{\beta_1}{\nu c}\right)^{\frac{1}{2}} \alpha(P_r)$$

where $\alpha(P_r)$ is a function of Prandtl number, P_r, tabulated by Goldstein (13).

For the fluid the unsteady equation is

$$\theta'' + P_r f(\eta)\theta' - \frac{i\omega P_r c}{\beta_1}\theta = 0$$

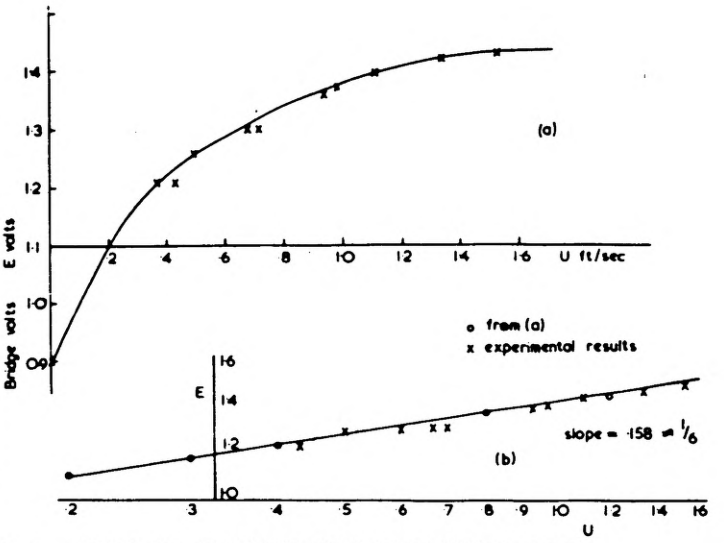

Fig. 1 LINEAR AND LOGARITHMIC PLOTS OF CALIBRATION CURVES

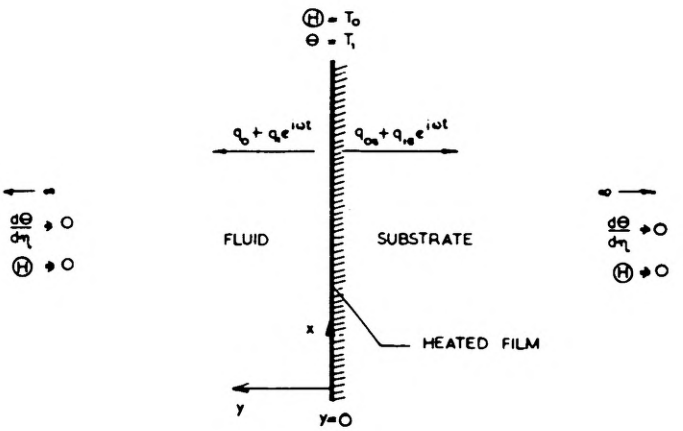

Fig. 2 THEORETICAL MODEL OF HEATED FILM

This equation has been solved numerically using a central difference technique.

It is assumed that the steady state temperature of the substrate is constant and we can write the frequency response of the heated film as

$$F = \frac{q_o}{q_o + q_1 + q_{1G}}$$

where the unsteady heat flux to the fluid is given by

$$q_1 = -k_f \frac{d|\theta|}{d\eta}\left(\frac{\beta_1}{\nu c}\right)^{\frac{1}{2}}$$

The frequency response is plotted on figure 3. In the paper by Bellhouse and Schultz[14] the variation of frequency response due to the dynamic heat transfer to the fluid is not included. The effect of the exclusion is shown on figure 3.

The importance of the positioning of the film on the substrate is shown to be of great importance if the results of this computation are compared with those of Bellhouse and Schultz. In their case they found it unnecessary to consider the dynamic heat transfer to the fluid whereas in this work it is shown to be of paramount importance. The choice of response applicable to a hot-film

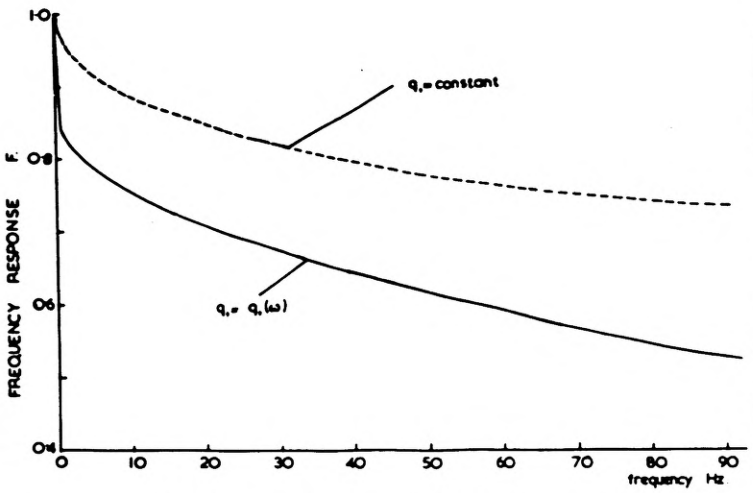

Fig. 3 THEORETICAL FREQUENCY RESPONSE OF HEATED FILM

probe depends on the construction of the probe itself. For the stagnation flow model to work the flow over the real probe must resemble stagnation flow. Fabula showed this to be the case for certain models of probe under certain working conditions which corresponded to those encountered in oceanic work.

The results show that the dynamic response of a heated film is less than the static calibration. Also that it is not valid to exclude the dynamic heat transfer to the fluid from calculations. It would also appear that the fall in the frequency response curve is not limited to fluids of low thermal conductivity as the values used in the above calculations were for a uniform stream of water approaching the film at 100 cm./sec.

A more complete discussion is given in reference 15.

THE TURBULENT WATER JET

Apparatus

The jet was produced by linking a 75 liter perspex water tank to a header tank through a 7.6 cm., internal diameter, duct. (figure 4). A 2.54 cm. nozzle was connected to the water tank end of the duct, giving a contraction ratio of about 10:1. The pressure head in the header tank was produced by inserting a 0.6 cm. nozzle between the header tank and the duct. Any unsteady flow created in the duct by the smaller nozzle was eliminated by smoothing its profile and inserting aluminum honeycomb, foam and nylon wool in the connecting duct. The level of water in the receiving tank was kept constant by means of a weir and a scavenge pump.

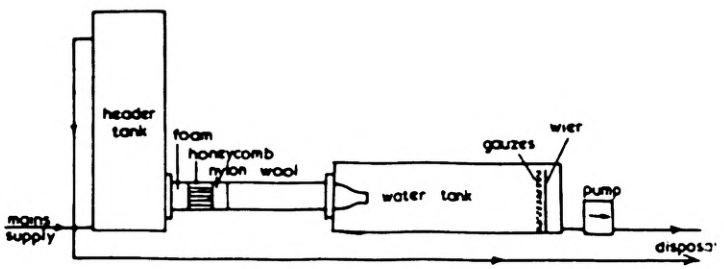

Fig 4 DIAGRAM OF EXPERIMENTAL RIG

The measurements were made using a hot-wire anemometer specially modified for use in water. The hot wires were made of 9 micron diameter tungsten wire, copper-plated at the ends, leaving 1.5 mm bare in the middle. The plated ends were soldered onto two conducting prongs, about 5 mm apart, on the end of the hot-wire probe. The probe was 15 cm. long and was connected to a length of low-noise coaxial cable by a Belling and Lee subminiature coaxial plug. The anemometer used was an I.S.V.R. constant temperature model. The probe was calibrated in a 15 cm. channel on the outer edge of a circular tank which could be rotated by a d.c. motor with a variable speed control. Using the calibration curve the hot-wire anemometer's lineariser circuit was set up according to the instructions in reference 16.

The frequency content of the signal from the anemometer with the probe in the turbulent water jet was known to be of low order so a Lockheed frequency modulated tape recorder No. 417 was used to record the signal. The recorder has a frequency response of within $\pm$ 0.5 dB of the reference input from 0-5000 Hz at a tape speed of 15 inches per second; the tape speed used in the experiments. The data were analyzed in the I.S.V.R. Random Data Analysis Center. A brief introduction to the facilities of the center is given by Mercer.[17]

Mean Velocity Measurements

The mean velocity profile of the jet found from a vertical traverse at one diameter downstream of the jet exit is shown in figure 5. (The results have been corrected for a 5° misalignment between the longitudinal axes of the jet and the traversing mechanism). It is interesting to note the peaks at $Z = \pm 1.0$ cm. The slight difference in magnitude of the peaks is probably due to the recirculation of the fluid in the collecting tank causing a retardation of the flow near the tank's base. The same peaks are visible in the horizontal traverse of the jet at two diameters downstream (figure 6). When dye was inserted upstream of the jet exit distinct vortices were visible under stroboscopic illumination flashing at about 10 Hz.

It is assumed in this report that the peaks on the mean velocity profiles are due to a continuous stream of vortices passing the measuring point giving a positive axial velocity internal to their center and a negative axial velocity externally. It is further assumed that the difference between the mean velocity profiles measured here and those where vortex shedding does not occur will give an indication of the velocity profile of the vortex. The non-vortex shedding profiles used are those measured by Laurence[18] which are at a similar Reynold's number to the present experiments. This velocity difference is plotted on figure 7. The existence of the peaks for both horizontal and vertical traverses of the jet taken with the flow visualization experiments suggested that the vortices were toroidal.

The velocity components of an error function toroidal vortex are given by Base.[19] If the vortex is centered around the x-axis as in figure 8, with axial dimensions of the vortex x_c and y_c and a core radius r_c, then if the position of the vortex is given by (ζ, η) relative to (x,y) and the circulation constant is Γ_c, the axial velocity component of velocity is given by,

$$u = B \left| 2 - \left(\frac{y}{y_c}\right) \left(\frac{y-\eta}{y_c}\right) \right|$$

where $$B = \frac{\Gamma_c}{\pi \eta} \left| \exp\left(-\frac{1}{2} \left(\frac{x-\zeta}{x_c}\right)^2 + \left(\frac{y-\eta}{y_c}\right)^2 \right) \right|$$

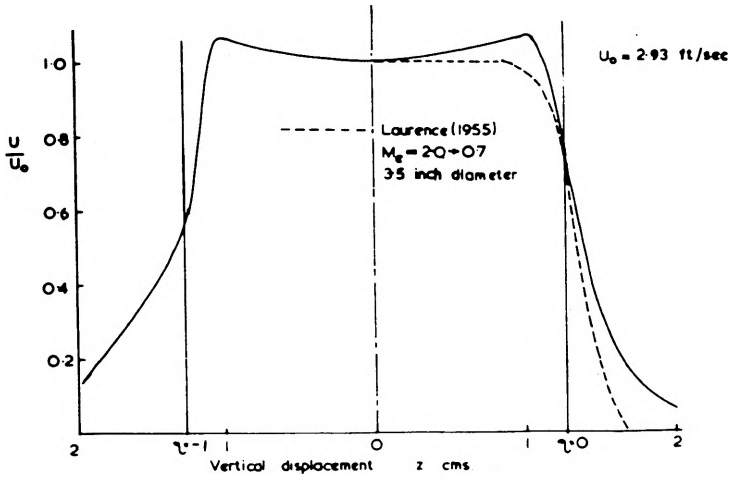

Fig 5 VERTICAL TRAVERSE OF JET AT X/D = 1

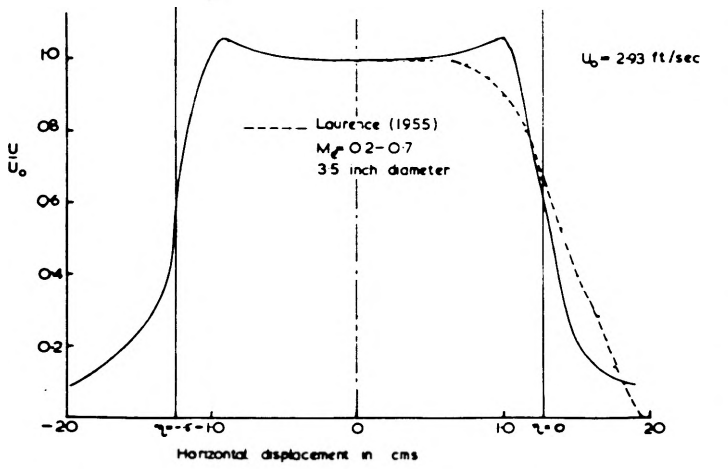

Fig 6 HORIZONTAL TRAVERSE OF JET AT X/D = 2

If we consider the axial component of velocity along a line x = $\hat{\xi}$ and assume a circular vortex ring, i.e. $x_c = y_c = r_c$. Then,

$$(u)_{x=\hat{\xi}} = \frac{c}{\hat{\eta}} \exp\left| -\frac{1}{2}(\hat{y}-\hat{\eta})^2 \right| \times \left| 2 - \hat{y}(\hat{y}-\hat{\eta}) \right|$$

where $\hat{y} = y/r_c$ and $\hat{\eta} = \eta/r_c$.

Completing the non-dimensionalization we have,

$$(\hat{u}) = \left(\frac{u.r_c.\pi}{\Gamma_c}\right) = \frac{1}{\hat{\eta}} \exp\left| -\frac{1}{2}(\hat{y}-\hat{\eta})^2 \right| \times \left| 2 - \hat{y}(\hat{y}-\hat{\eta}) \right|$$

By taking r_c as the distance between the zero velocity point A, on the vortex velocity profile, and the peak in the experimental results and $\hat{\eta}$ as the distance from the jet axis to the zero vortex velocity point, the values of $(\hat{u})$ were calculated for different values of $\hat{y}$. These were plotted as a ratio of the maximum values of $(\hat{u})$ against $\hat{y}$ on figure 7. The slight shift noticeable between the calculated curve and the experimental results is due to the fact that the core of the toroidal vortex has a finite velocity due to self-translation of the vortex and so is not situated at the zero vortex velocity point. By changing the value of $\hat{\eta}$ another curve is plotted which takes account of this self-translation and the calculations and experimental results fit very closely, figure 7.

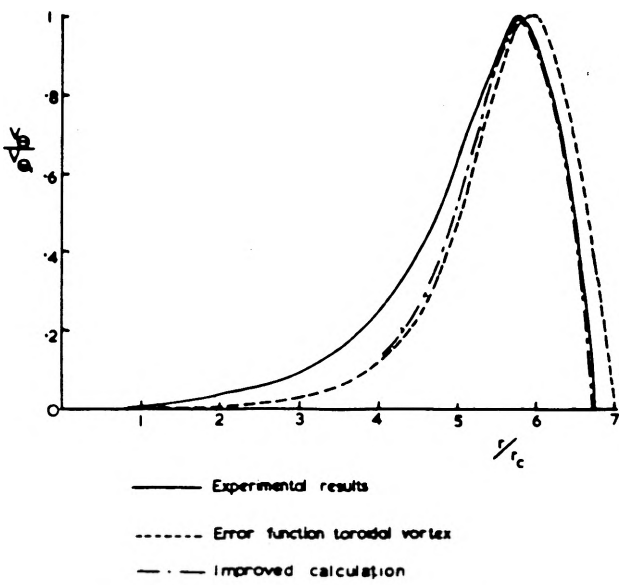

COMPARISON OF VORTEX VELOCITY PROFILES

Fig. 7

From the experiments the maximum value of velocity at the core was estimated to be 5.36 cm./sec. The core radius was estimated to be 0.175 cm. Thus when,

$$\hat{y} = \hat{\eta}$$

$$\Gamma_c = \frac{u.r_c.\pi}{2} = 9.46 \text{ cm.}^2/\text{sec.}$$

That is, the circulation constant of the toroidal vortex is 9.46 cm./sec. The comparison between the toroidal vortex shape and experimental results has only been made over the interior of the vortex where the velocity measurements were steady.

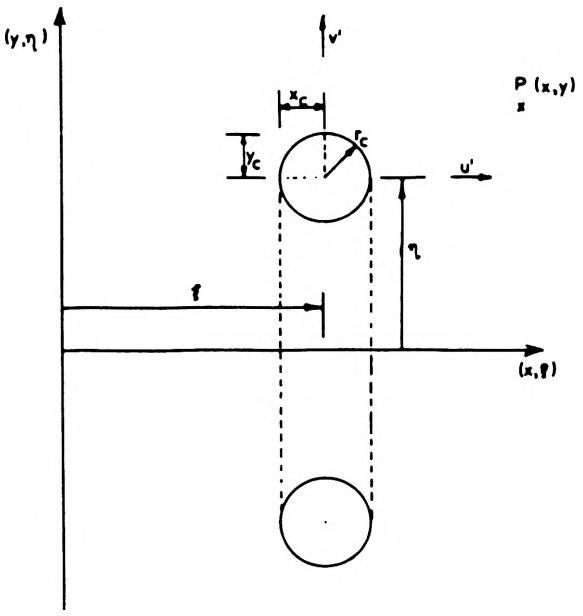

COORDINATES AND DIMENSIONS OF ERROR FUNCTION TOROIDAL VORTEX

Fig. 8

Spectrum Measurements

The spectra of the fluctuating u-component of velocity measured at X/D = 1 and 3 at y = 0.1 for various jet exit velocities are shown in figures 9 and 10, respectively. It is noticeable that a very large peak occurs at about 10 Hz one diameter downstream and at 5 Hz three diameters downstream. Bradshaw[20] connected this frequency halving with a sharp maximum in Reynolds shear stress and it is at this point he says "according to Wille, confluence of vortex rings occur". In his own experiments with a Reynolds number based on jet diameter of 3.5×10^5 Bradshaw showed that the distance to frequency halving was 1.02 cm. He also noted that when the free stream speed is doubled the distance from the jet exit to the point of maximum u-component intensity decreased by a factor of $1/\sqrt{2}$. Although, as Bradshaw points out, this could be a dependence on the boundary layer thickness in the pipe it could also suggest a dependence of the flow on $(Re)^{-\frac{1}{2}}$. In the author's experiments with a Reynold's number of 1.9×10^4 the assumption of a "pseudo-laminar" initial region of the jet, i.e. a dependence on $(Re)^{-\frac{1}{2}}$, gives the distance to frequency halving as 4.34 cm. or X/D = 1.7. This is compatible with the experimental values obtained.

There is a further way of interpreting the spectrum measurements made in the jet. If the flow upstream of the jet exit is unsteady then the jet exit would be presented with a varying mass flow with a fundamental wavelength of 2D (see figure 11(a)). The characteristic frequency connected with this unsteadiness would be the flow velocity divided by the wavelength, 2D, viz

$$f_o = \frac{U_o}{2D}$$

The results of a number of experimenters have been used to compare the peak in

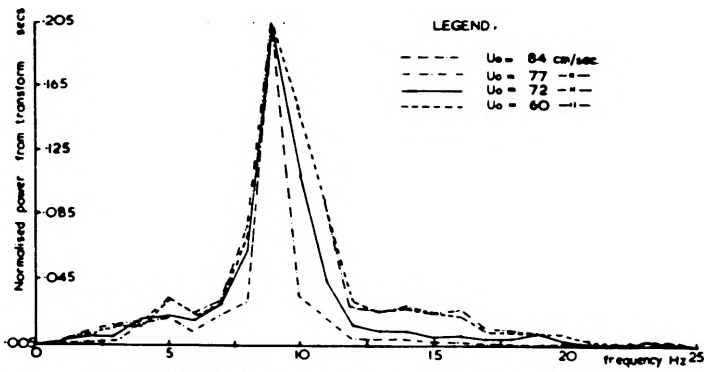

TURBULENCE SPECTRA AT X/D=1, η=·01 FOR VARIOUS EXIT VELOCITIES
Fig.9 (Output from Myriad II processor and A to D converter)

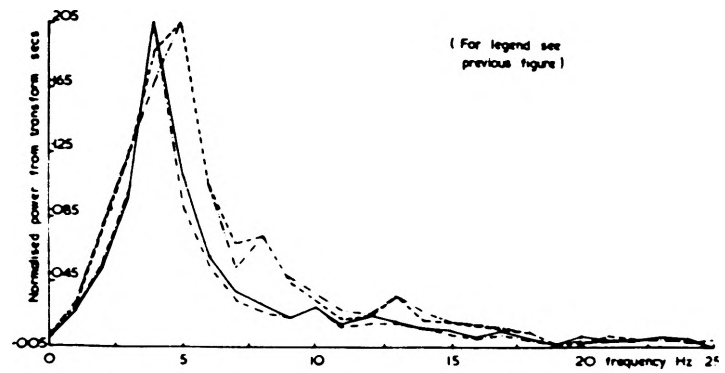

TURBULENCE SPECTRA AT X/D=3, η=·01 FOR VARIOUS EXIT VELOCITIES
Fig 10 (Output from Myriad II processor and A to D converter)

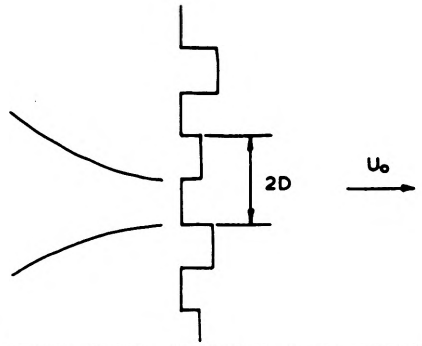

11(a) CHARACTERISTIC UNSTEADY FLOW FREQUENCY

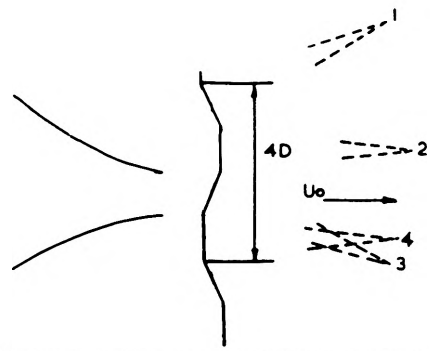

11 (b) CHARACTERISTIC VORTEX RING FREQUENCY

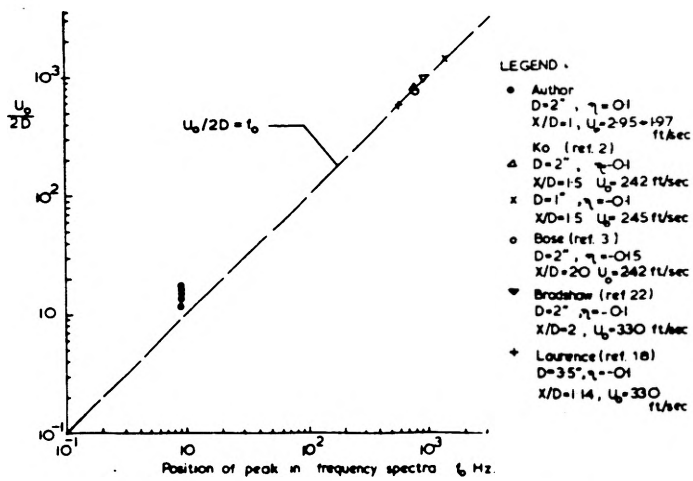

Fig 12 COMPARISON OF PEAK FREQUENCY IN TURBULENCE SPECTRUM AND THE CHARACTERISTIC MONOPOLE FREQUENCY, $U_o/2D$ X/D=1→2

the spectrum measurements, close to the jet exit, with this characteristic frequency. The frequency peak is plotted against Uo/2D in figure 12, and the correlation is nearly exact.

It can be seen that the position of the peak frequency at X/D = 1 does not vary visibly with exit speed. It is possible that, at these low velocities, a phenomenon is occurring similar to that reported by Becker and Massaro.[21] The frequency of a pure tone giving maximum excitation of the jet, in their experiments, was constant for finite Reynold's number ranges. This occurred at very small Reynold's numbers but, as is suggested by the frequency spectra given here, a low flow speed may produce the same effect.

Jet Structure

The initial section of the jet mixing region was discussed in the previous section. It was concluded that the length of this "pseudo-laminar" region was

dependent on the inverse square root of Reynolds number. The transition from this region to the fully developed shear flow occurs, according to Bradshaw's flow visualization pictures, through the longitudinal vortices. The properties of the mixing zone, which surrounds the potential core, have been described adequately elsewhere, i.e. references 1 and 22.

The potential core, which lies inside the mixing layer, and terminates at X/D about 4.5, does not appear to have a constant angle of dimination. If the point of maximum turbulence intensity, taken from the measurements of Laurence[17] and Bose[3], is plotted as a function of radial displacement there is a definite inward displacement at X/D = 3 (figure 12). If the tail of the potential core were shaking then this would cause a stretching of the potential core about the center of rotation of the shaking tail. It would appear, by considering figure 12, that the last one and a half diameters length of the potential core are shaking - probably because of the random arrival of vortex rings, shed from the jet lip, causing a variable pressure on each side of the tail of the potential core. It has been reported by Wilkinson[23] that the vortex rings were not shed from the jet lip in the plane of the jet, neither was there any spiralling motion. The only other possibility being that the vortex rings were shed "at random angles to the jet axis". The fundamental wavelength of such disturbances would be 4D (see figure 11(b)). The results of various researchers have been used to plot the position of the peak in the frequency spectrum near the tail of the potential core against a characteristic frequency Uo/4D. The results, figure 13, show a close relationship for various jet dimensions and velocities. So it would appear that there may be a transverse oscillation of the tail of the potential core.

The production of distinct vortex rings at the jet lip as has been noted in these experiments has also been noticed in air jets with large contraction ratios such as Bradshaw's jet[21] with a ratio of 36:1. This occurrence may be explained in terms of the way in which information is fed from one part of the flow to another. In the water jet experiments the flow is almost completely incompressible. So any change in conditions at a single point in the flow will be felt immediately everywhere else in the fluid. If a vortex ring or discontinuity occurs at the jet exit this discontinuity will create a potential field which will be felt at all points in the flow including upstream of the nozzle. This will cause an acceleration of the flow upstream allowing the vortex to complete its formation. When the vortex breaks away from the lip the flow will be retarded creating a further discontinuity and repeating the process. For large contraction ratio nozzles a similar process applies but in this case the immediacy of information transmission upstream of the jet is facilitated by the fluid amplification effect of the low velocity head upstream. When there is no large contraction ratio or the fluid is compressible then there is a time lag in information transmission so the vortices may not be given the maximum time to develop.

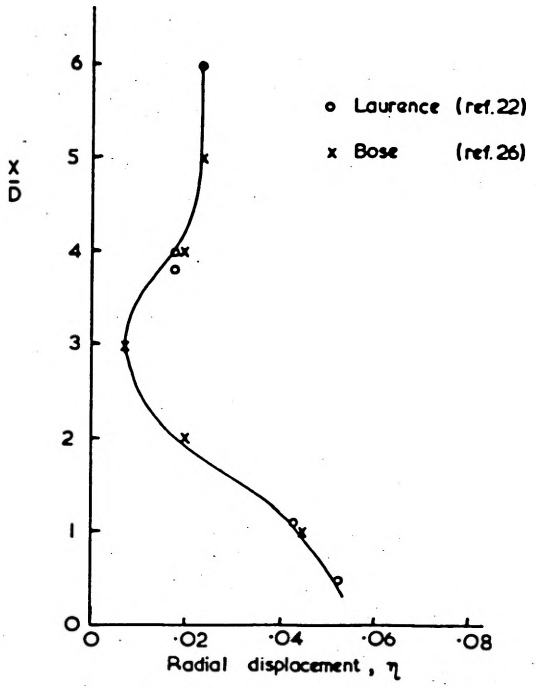

RADIAL DISTRIBUTION OF POSITION OF PEAK AXIAL TURBULENCE INTENSITY WITH AXIAL DISTANCE

Fig.13

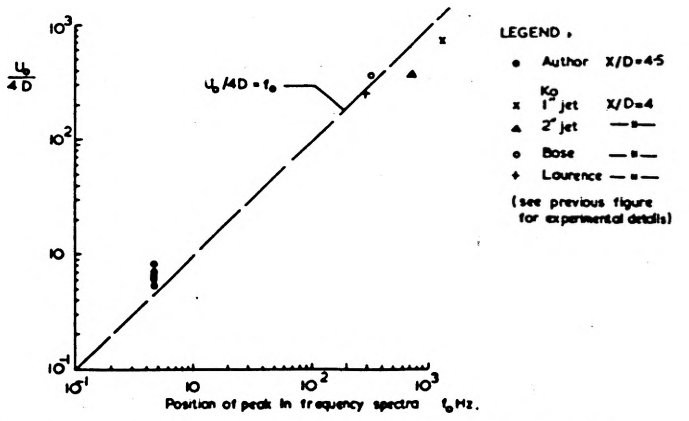

Fig.14 COMPARISON OF PEAK FREQUENCY IN TURBULENCE SPECTRUM AND THE CHARACTERISTIC FREQUENCY, $U_0/4D$ X/D 4 and 4·5

CONCLUSIONS

The main purpose of this report was to investigate the structure of a turbulent water jet.

By considering the difference between the velocity profiles of Laurence and those made in water it was possible to show that the vortices shed from the jet lip were error function toroidal vortices.

The peak in the spectrum measured at X/D = 1 was compared with a characteristic frequency Uo/2D and was found to be in close agreement as were the results of other researchers. The potential core of the jet was shown to have a contraction at X/D = 3 and this was associated with a shaking of the tail of the potential core caused by the shedding of vortices at various angles from the jet lip.

The production of discrete toroidal vortices in the water jet and large contraction ratio air-jets was connected with the ability of the fluid to transmit information from one point in the fluid to another with no time lag.

ACKNOWLEDGMENTS

I wish to express my thanks to Dr. P.O.A.L. Davies for his ideas on vortex production and his helpful supervision of this work. I would like also to thank the Science Research Council for supporting me during this work.

SYMBOLS

B	function of vortex circulation constant
D	thermal diffusivity
D_f	thermal diffusivity in fluid
D_s	thermal diffusivity in substrate
F	frequency response of heated film
k	thermal conductivity
k_f	thermal conductivity in fluid
k_s	thermal conductivity in substrate
Pr	Prandtl number
$\bar{q}$	velocity vector
q_o	steady heat transfer to fluid
q_1	unsteady heat transfer to fluid
q_{1G}	unsteady heat transfer to substrate
r_c	core radius of vortex
t	time
T	temperature
T_o	steady temperature at interface
T_1	fluctuating magnitude of temperature at interface
u	axial component of vortex velocity
$\hat{u}$	non-dimensional velocity
U_o	jet axial velocity
v	velocity approaching wall
x	coordinate parallel to interface
x_c, y_c	axial dimensions of vortex
X	jet axis coordinate
y	coordinate normal to interface
$\hat{y}$	non-dimensional radial coordinate
$\alpha(Pr)$	function of Prandtl number
$f_{1/c}$	ratio of normal velocity to distance from stagnation point
η	radial position of core of vortex
$\hat{\eta}$	nondimensional η
ξ	axial position of vortex
Γ_c	circulation constant of vortex
θ_s	time average component of temperature
θ	magnitude of fluctuating component of temperature
ω	angular frequency
ν	kinematic viscosity

Subscripts

f	in the fluid
s	in the substrate

REFERENCES

1. Davies, P.O.A.L., Fisher, M.J. and Barrett, M.J., "Turbulence in the Mixing Region of a Round Jet", J. Fluid Mech., 15, 337 (1963).
2. Davies, P.O.A.L., Ko, N.W.M., and Bose, B., "The Local Pressure Field of a Turbulent Jet", A.R.C., C.P. 989, 1968.
3. Bose, B., "Turbulence Measurements in Air Jets", Ph.D. Thesis, University of Southampton, 1968.
4. Gandaghran, E., "A New Instrument for Velocity Measurements in Water Under Turbulent Conditions", Mittsilungen des Hydraulischen Institutes - T. H. Munich, 4 (1931).
5. Worster, R.C., "Practical Problems in Using the Hot-wire Anemometer in Water", B.H.R.A., T.N.2. (1948).
6. Jones, D., Burkett,D.J., and Welham, D., "A Technique for Continually Cleaning Hot-wire Probes for Measuring Turbulence in Water", ARL/RI/G/IN/19/6, Admiralty Research Lab. Report, 1959.
7. Delleur, J.W., Toebes, G.N., and Liu, C.L., "Hot-wire Physics and Turbulence Measurements in Liquids", Tech. Rep. No. 13, Purdue University, 1966.
8. Morris, P. J., "Temperature Compensation of a Hot-wire", Proceedings of a Symposium on Instrumentation and Data Processing for Industrial Aerodynamics", Paper 8, National Physical Laboratory, November 1968.
9. Morris, P.J., "Measurements and Flow Visualization in a Water Jet", Honors Thesis, Southampton University, 1967.
10. Bankoff, S.G., and Rosler,R.S., "Constant Temperature Hot-film Anemometer as a Tool in Liquid Turbulence Measurements", Rev. Sci. Instr., 33, 1209 (1962).
11. Fabula, A.G., "Dynamic Response of Towed Thermometers", J. Fluid Mech., 34, 449 (1968).
12. Curle, N., "The Laminar Boundary Layer Equations", Oxford Math. Monographs, 1962.
13. Goldstein, S., "Modern Developments in Fluid Dynamics", Oxford Univ. Press, 1938.
14. Bellhouse, B.J., and Schultz, D.L., "The Determination of Fluctuating Velocity in Air with Heated Thin Film Gauges", J. Fluid Mech., 29, 289 (1967).
15. Morris, P.J., "The Structure of a Turbulent Water Jet", M.Sc. Thesis, University of Southampton, 1968.
16. Wold, I., and Mason, J., "Simplified Operating Instructions for the I.S.V.R. Constant Temperature Hot-wire Anemometer", I.S.A.V. Memorandum, 187, 1967.
17. Mercer, C., "Introduction to the I.S.V.R. Random Data Analysis Center", I.S.A.V. Memorandum, 209, 1967.
18. Laurence, J.C., "Intensity, Scale, and Spectra of Turbulence in the Mixing Region of a Free Subsonic Jet", N.A.C.A. T.N. 3561, 1955.
19. Base, T.E., "Computer Studies of Vortex Models to Represent Turbulent Fluid Flow", Ph.D. Thesis, University of Southampton, 1969.
20. Bradshaw, P., "The Effect of Initial Conditions on the Development of a Free Shear", J. Fluid Mech., 26, 225 (1966).
21. Becker, H.A., and Massaro, T.A., "Vortex Evolution in a Round Jet", J. Fluid Mech., 31, 435 (1968).
22. Bradshaw, P., Ferriss, D.N., and Johnson, R.F., "Turbulence in the Noise Producing Region of a Turbulent Jet", J. Fluid Mech., 19, 591 (1964).
23. Wilkinson, R., "An Investigation of the Turbulence Near the Orifice of a 2-Inch Cold Air Jet", M.Sc. Thesis, Southampton University, 1966.